Heterologous Expression of Marine Bacterial Alkaline Phosphatase Enhances Abiotic Stress Tolerance and Metabolic Adaptation in Tobacco

Yulia Yugay[1] · Olesya Kudinova[1] · Elena Vasyutkina[1] · Peter Adedibu[2] · Dina Rudenko[1] · Egor Alaverdov[1] · Tatiana Rusapetova[1] · Alexandra Fialko[1] · Veronika Degtyareva[1] · Victor Bulgakov[1] · Larissa Balabanova[3] · Yury Shkryl[1]

Abstract

Phosphorus is essential for plant growth, yet its availability in soils is often limited, necessitating phosphorus fertilizers derived from non-renewable resources. This study reports the first successful heterologous expression of the alkaline phosphatase gene (*CaAP*) from the marine bacterium *Cobetia amphilecti* in transgenic *Nicotiana tabacum*. Transgenic lines exhibited enhanced resilience to salt and osmotic stress, as demonstrated by up to 30% higher germination rates, fivefold longer root lengths, and improved membrane stability compared to wild-type (WT) plants. These benefits were linked to increased antioxidant enzyme activity, reduced reactive oxygen species (ROS) levels, lower malondialdehyde (MDA) content, decreased electrolyte leakage, and better maintenance of relative water content. Biochemical analyses revealed significant 1.5- to twofold increases in total phenolic and flavonoid content, along with a marked rise in proline accumulation, suggesting broader metabolic reprogramming. Gene expression profiling confirmed upregulation of key stress-related genes (e.g., *SOD*, *CAT*, *PHT1*, *NHX*, *CHS*, *P5CS*) and downregulation of *CDPK*, indicating *CaAP's* role in transcriptional regulation. However, transgenic plants exhibited reduced performance under calcium-deficient conditions, likely due to the enzyme's calcium dependence, highlighting a trade-off in low-Ca^{2+} environments. These findings underscore the biotechnological potential of marine bacterial phosphatases for engineering stress-resilient crops while identifying critical limitations linked to nutrient context. Further field trials are required to assess the viability of this approach under real-world agricultural conditions.

Graphical abstract
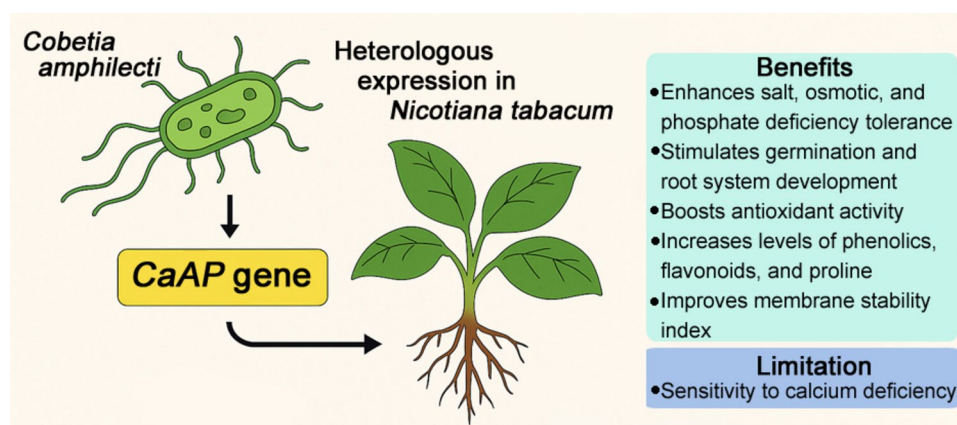
Handling Editor: Jose M. Mulet.

Extended author information available on the last page of the article

Introduction

Abiotic stresses such as drought, salinity, and nutrient and temperature extremes significantly impair physiological processes in plants, including photosynthesis, nutrient uptake, and water regulation, ultimately reducing agricultural productivity (Solis et al. 2022). Enhancing plant resilience to these stressors is crucial for sustainable crop production in the face of climate change and a growing global population.

Phosphorus is an indispensable macronutrient for plant growth, and its deficiency severely impacts crop health and agricultural productivity (Gerke 2024). In its oxidized form, phosphorus is an integral component of various biomolecules, including nucleic acids, phospholipids, and secondary messengers, that are critical to cellular function. Plants primarily acquire phosphorus in the form of inorganic phosphate (Pi), which is essential for numerous metabolic and energy transfer processes (Khan et al. 2023). Consequently, phosphorus-based fertilizers have become a cost-effective and widely adopted method to boost plant productivity. However, these fertilizers are derived from finite rock phosphate reserves, which are projected to be depleted within the next 70 to 100 years—or sooner if consumption accelerates beyond current estimates. Despite their widespread application, plants absorb less than one-third of the phosphorus supplied through fertilizers, primarily due to several limiting factors (Gerke 2024; Makris et al. 2023). First, phosphate tends to react with soil components, forming insoluble complexes that are unavailable for plant uptake. Second, soil microorganisms rapidly convert phosphate into organic forms, which plants are generally unable to metabolize efficiently. Third, phosphorus fertilizers often encourage the growth of weeds, thereby intensifying competition for available nutrients and further reducing the bioavailability of phosphorus for crops. These inefficiencies lead to significant phosphorus losses, necessitating the excessive application of fertilizers to maintain crop yields (Lambers et al. 2023). However, this practice increases agricultural costs and contributes to environmental issues such as soil degradation and the eutrophication of water bodies.

C. amphilecti is a marine bacterium that thrives in highly saline and nutrient-poor environments, making it a promising source of stress-resistance genes (Balabanova et al. 2016). It produces robust enzymes, including alkaline phosphatases (APs), which remain active under high pH and salt stress conditions (Adedibu et al. 2024). APs catalyze the hydrolysis of phosphate esters, releasing inorganic phosphate that can be readily utilized by plants. The heterologous expression of microbial *AP* genes has emerged as a promising strategy to enhance phosphorus utilization efficiency in plants. Marine bacteria, in particular, are a valuable but underexplored reservoir of stress-tolerant enzymes, including APs, due to their adaptation to nutrient-deficient and extreme environments. Unlike acid phosphatases, APs exhibit specificity for phosphorothioate acid monoesters containing sulfur substitutions rather than oxygen substitutions (Coleman 1992).

We propose that the unique substrate specificity and functional features of APs make them strong candidates for improving plant stress tolerance. Despite their potential, the role of marine bacterial APs in plants remains unexplored. Expression of the *CaAP* gene was found to enhance plant resilience to salt and osmotic stress, likely through improved antioxidant defense, reduced ROS accumulation, and metabolic reprogramming. At the same time, *CaAP*-expressing plants are highly sensitive to calcium deficiency, highlighting a limitation associated with the calcium dependence of the enzyme. The study provides insight into AP-mediated stress responses and supports the development of improved crop stress tolerance strategies.

Materials and Methods

Gene Cloning and Construction of Binary Vector

The complete sequence of the *CaAP* gene was amplified through PCR using specific primers: forward primer CaAP-D (5′-TAT GGT CTC AAA AAA TGG CAG AGA TCA AGA ATG TCA TTC-3′) and reverse primer CaAP-R (5′-TAT GGT CTC TAG CGC TAG CGT CAA TGG TGA TGG TGA TGG TGC TTC GCT ACC ACT GTC TTC-3′), as outlined in a prior study (Adedibu et al. 2024). PCR was performed for 35 cycles using the following parameters: 95 °C for 30 s, 58 °C for 30 s, and 72 °C for 1 min 30 s. The resulting amplified fragment was inserted into the pHREAC vector at BsaI restriction sites, under the control of the 35S CaMV promotor and NOS terminator, creating the pHREAC-CaAP construct with no additional modifications. DNA sequencing was performed to verify that the construct was free from mutations. Subsequently, the validated pHREAC-CaAP construct was introduced into *Agrobacterium tumefaciens* strain EHA105/pTiBo542 (Hood et al. 1993) using the GenePulser Xcell™ electroporation system (Bio-Rad Laboratories, Inc., Hercules, CA, USA), adhering to the instructions provided by the manufacturer.

Transformation of Tobacco and Generation of Transgenic Plants

Sterile leaf explants of *N. tabacum* L. were infected using *A. tumefaciens* harboring the pHREAC-CaAP plasmid. The infected leaf discs were co-cultivated with *A. tumefaciens*

for 48 h and subsequently transferred onto White's solid medium (White 1954) containing 2 mg/L 6-benzylaminopurine, 0.1 mg/L α-naphthaleneacetic acid (Degtyarenko et al. 2024), 500 mg/L cefotaxime, and 400 mg/L kanamycin. Within three days of subculture, the edges of the explants showed bulging. After a culture duration of four weeks, with transfers to fresh medium every eight days, somatic embryos resistant to kanamycin were obtained. These embryos were then subcultured on the same regeneration medium for further development. Following three selection cycles, cotyledonary-stage embryos were moved to White's solid medium without added hormones to facilitate elongation and rooting. Two independent transgenic lines, designated as Nt-CaAP1 and Nt-CaAP2, were selected from a larger pool of kanamycin-resistant transformants and used for further analysis. The selection was based on confirmed transgene integration by PCR and consistently high expression levels of AP.

Isolation of cDNA and Real-Time PCR Analysis

Total RNA isolation and first-strand cDNA synthesis were performed following a previously described protocol (Balabanova et al. 2022). Detached leaves of *N. tabacum* were utilized to assess the expression levels of *CaAP* mRNA. Three biological replicates, derived from separate RNA extractions were included in the analysis with each biological replicate assessed in three technical replicates. Quantitative real-time PCR (qPCR) was conducted using the Bio-Rad CFX96 Real-Time System (Bio-Rad Laboratories, Inc., Hercules, CA, USA) and 2×BioMaster RT-PCR SYBR Blue (Biolabmix®, Novosibirsk, Russia), as detailed previously (Shkryl et al. 2022). The specific primers used for qPCR are listed in Supplementary Table S1. Amplification efficiencies for all primer pairs ranged between 96 and 100%, as determined by standard curve analysis. The *β-actin* gene of *N. tabacum* served as internal reference control. Relative gene expression was calculated using the $2^{-\Delta\Delta Ct}$ method. Data analysis was carried out using CFX Manager Software (Version 3.1; Bio-Rad Laboratories).

Seed Germination Under Stress Conditions

Seed germination was assessed according to a previously established protocol (Leubner-Metzger et al. 1995). In short, approximately 50 seeds were surface-sterilized (Lindsey et al. 2017) and then placed into specific sections of 90-mm Petri dishes containing White's solid medium, which was supplemented with various stress conditions such as phosphate deficiency, excess phosphates, 100 mM NaCl, 100 mM mannitol, or calcium deficiency. The Petri dishes were incubated agar side down in a climate chamber set to 24 °C with a photosynthetic photon flux density (PPFD) of 150 µmol m^{-2} s^{-1} and a 6-h light/8-h dark photoperiod.

Germination was monitored daily by counting the number of seeds that had germinated, defined as the appearance of the radicle and two cotyledons. For each transgenic line, three replicates of 50 seeds were used, and the data were represented as the cumulative percentage of germinated seeds across all trials.

Root System Development Under Abiotic Stress Conditions

Tobacco seeds were surface-sterilized and seeded into square Petri dishes containing White's solid medium supplemented with phosphates deficit or abundant, 100 mM NaCl, 100 mM mannitol, calcium deficit in groups of 10 seedlings from each line. The dishes were incubated at an angle of 30° from the vertical in the growth chamber for 4 weeks at of 24 °C and 150 µMol m^{-2} s^{-1} PPFD, with a 16/8 light/dark photoperiod. To measure root length, the agar was softened by heating to 80 °C in a water bath, the root system was carefully isolated from the growth medium, and the length of the primary (longest) root was measured with a ruler. Three replicates, each consisting of 10 plants per line, were maintained.

Peroxidase Activity Determination

Fresh tissue (500 mg) from each sample was homogenized in a pre-chilled mortar with ice-cold extraction buffer (50 mM Tris–Cl, pH 7.5). The mixture was centrifuged, and the resulting supernatant was collected for analysis. Total specific peroxidase activity was measured using the spectrophotometric method described by Ferrer et al. (1990), with slight modifications. The reaction mixture contained 50 mM Tris–HCl (pH 7.5), 5 mM 4-methoxy-α-naphthalol as the electron donor substrate, and 0.33 mM H$_2$O$_2$ as the co-substrate. The reaction was initiated by adding 100 µL of the enzyme extract and carried out at 25 °C. The formation of the colored product was monitored for 1 min at 593 nm using a Benchmark Plus microplate spectrophotometer. Peroxidase activity was calculated in nkat using the extinction coefficient ($\varepsilon_{593} = 2.1 \times 10^4$ nkat M^{-1} cm^{-1}) for the absorption differences. One nanokatal (nkat) is defined as the amount of enzyme that converts 1 nmol of substrate per second under the assay conditions. Four independent extractions, each with two technical replicates, were performed for each sample.

Hydrogen Peroxide Content Analysis

The potassium iodide (KI) method (Junglee et al. 2014) was used to determine hydrogen peroxide levels in tobacco leaves. In brief, 100 mg of leaf tissue was immediately ground in liquid nitrogen. For simultaneous extraction and

colorimetric reaction, 250 µl of 0.1% (w/v) TCA, 250 µl of 10 mM potassium phosphate buffer (pH 7.0), and 500 µl of 1 M KI were added to the homogenized tissue, and the mixture was incubated at 4 °C for 10 min. For each sample, a control was prepared by substituting KI with water in the buffer. To minimize light exposure during the procedure, samples and solutions were handled under reduced light conditions. The homogenate was centrifuged at $15,000 \times g$ for 10 min at 4 °C, and 200 µl of the resulting supernatant was transferred to a 96-well plate. The hydrogen peroxide content was measured using a Benchmark Plus microplate spectrophotometer (Bio-Rad Laboratories) based on a standard curve.

Measurement of Lipid Peroxidation

Lipid peroxidation in control and transgenic plant samples was analyzed by quantifying malondialdehyde (MDA), a key product of lipid peroxidation. MDA levels were determined using the thiobarbituric acid (TBA)-based method described by Buege and Aust (1978). Fresh samples (100 mg) were homogenized in 1 ml of TBA reagent, which contained 20% trichloroacetic acid (TCA), 0.5% TBA, and 2.5 N HCl. To minimize interference caused by iron released during homogenization, ethylenediaminetetraacetic acid (EDTA) was added at a final concentration of 10 mM. The homogenized mixture was incubated in a boiling water bath for 20 min and then centrifuged at $10,000 \times g$ for 5 min to remove flocculent materials. The absorbance of the clear supernatant was measured at 535 nm using a Benchmark Plus microplate spectrophotometer (Bio-Rad Laboratories), with a blank sample (containing no plant material) serving as the reference.

Free Radical Scavenging Analysis

The antioxidant activity of plant extracts was assessed using the 2,2-diphenyl-1-picrylhydrazyl (DPPH) free radical scavenging method, as described by Shkryl et al. (2023). Following 30 min of incubation at 24 °C, the absorbance of the control sample (A1, containing an equivalent amount of DPPH solution) and the test extracts (A2) was measured at 518 nm using a Benchmark Plus microplate spectrophotometer. A blank solution, consisting of plant extract in ethanol without DPPH, was used as the reference. The percentage inhibition (%in h) of free radicals was calculated using the formula:

$$\%\text{in}h = \frac{= (A1 - A2)}{A1} \times 100\%$$

The IC_{50} values, indicating the concentration of extract required to achieve 50% free radical scavenging activity, were determined through linear regression of the relationship between the percentage of antioxidant activity and the extract concentration.

Membrane Integrity and Electrolyte Leakage

Relative electrolyte leakage (REL) was assessed following the procedure outlined by Blum and Ebercon (1981) and used as an indicator of membrane permeability and stress-induced cellular damage. Approximately 100 mg of fresh leaves were thoroughly rinsed with deionized water three times to remove surface impurities and then submerged in 30 mL of deionized water for 2 h. The first conductivity measurement (C1) was taken using a conductivity meter. After boiling the samples for 10 min, the second conductivity measurement (C2) was made. The relative electrolyte leakage (REL) was calculated using the formula:

$$REL = \left(\frac{C1}{C2}\right) \times 100\%$$

For measuring the membrane stability index (MSI), the technique described by Onwueme (1979) was used to evaluate the structural integrity of cell membranes under stress conditions. Samples were incubated at 40 °C for 30 min before the first conductivity measurement (C1). After boiling for 10 min, the second conductivity measurement (C2) was recorded. The MSI was calculated using the formula and presented as a percentage:

$$MSI = \left(1 - \frac{C1}{C2}\right) \times 100\%$$

Relative Water Content

To determine relative water content (RWC), freshly excised leaves were immediately weighed to obtain the fresh weight (FW). The leaves were then placed in a plastic container lined with multiple layers of filter paper, which was moistened with distilled water to ensure hydration. The samples were left at 4 °C for 7 h for full hydration. After this period, the leaf surfaces were gently blotted with filter paper to remove excess water, and the turgid weight (TW) was recorded. The leaves were then dried following the method described by Huang et al. (2019), and the dry weight (DW) was measured. The RWC was calculated using the formula: and presented as a percentage:

$$RWC = \left(\frac{FW - DW}{TW - DW}\right) \times 100\%$$

Free Proline Content

Free proline content was measured using the method described by Bates et al. (1973). One gram of leaf material was homogenized in 10 mL of 3% sulfosalicylic acid, and the resulting homogenate was centrifuged at $12{,}000 \times g$ for 20 min at room temperature. The supernatant (2 mL) was mixed with 2 mL of glacial acetic acid and 2 mL of acid ninhydrin reagent. The reaction mixture was incubated at 100 °C for 1 h. After the incubation, the reaction was stopped by placing the tubes in an ice bath. To extract the chromophore, 4 mL of toluene was added to each tube. The absorbance of the toluene layer containing the chromophore was measured at 520 nm. Proline concentration was calculated from a standard curve using L-proline. The results were expressed as micrograms of proline per gram of fresh weight.

Determination of the Total Phenolic Content

The total phenolic content (TPC) of tobacco extracts was determined using the Folin–Ciocalteu method, with slight modifications as described in the protocol by Singleton et al. (1999). To 25 μL of extract, 25 μL of Folin–Ciocalteu's reagent (diluted 1:3 with water) was added, and the mixture was incubated for 5 min at 25 °C in a 96-well plate. Subsequently, 200 μL of water and 25 μL of 10% sodium carbonate were added to dilute the solution, and the mixture was incubated for an additional 1 h. The absorbance was then measured at 725 nm using a microplate reader. A standard curve was constructed using gallic acid (0–200 μg/mL in ethanol). The TPC was expressed as milligrams of gallic acid equivalents per gram of dry weight.

Determination of the Total Flavonoid Content (TFC)

The total flavonoid content was measured by the $AlCl_3$ colorimetry-based method (Peng et al. 2019). The tobacco extract (80 μL) was mixed with 80 μL of 2% aluminum chloride and 120 μL of 50 g/L sodium acetate (water solution) in a 96-well plate, followed by 2.5 h of incubation at 25 °C. The absorbance at 440 nm was measured in a microplate reader, and quercetin methanolic solution (0–50 μg/mL) was added for standard curve generation. Each sample was processed in triplicate, and the result was presented in mg quercetin equivalents.

Statistical Analysis

All values are expressed as the mean $\pm$ SE. Data normality was verified using the Shapiro–Wilk test. For statistical evaluation, the Student's t test was used to compare the two independent groups. For comparison among multiple data, analysis of variance (ANOVA) followed by a multiple comparison procedure was employed. Fisher's protected least significant difference (PLSD) post hoc test was employed for the inter-group comparison. The level of statistical significance was set at $p \leq 0.05$. All experiments were performed with at least three independent biological replicates.

Results

Generation of Transgenic Tobacco Lines Expressing the *CaAP* Gene

To investigate the impact of AP on plant tolerance to abiotic stresses, transgenic tobacco lines (Nt-CaAP1 and Nt-CaAP2) were developed, expressing the *CaAP* from the marine bacterium *C. amphilecti*. The *CaAP* gene was amplified from the genomic DNA of *C. amphilecti* and cloned into the binary vector pHREAC. The resulting construct, pHREAC-CaAP (Fig. 1A), was introduced into *Agrobacterium tumefaciens* strain EHA105 using electroporation.

Using Agrobacterium-mediated transformation of *N. tabacum* plant explants (Fig. 1B). Primary calluses were generated and subsequently induced to regenerate whole plants on White's solid medium supplemented with 2 mg/L naphthylacetic acid, 0.1 mg/L benzylaminopurine, cefotaxime 400 mg/L and 400 mg/L kanamycin (Fig. 1C). Figure 1D shows the stage of elongation of regenerated shoots and induction of root development on White's solid medium without growth regulators. This stage ensures the development of full-fledged seedlings. Then DNA was extracted from the regenerated plants to confirm the transgenic status, and PCR analysis was performed to verify the presence of the transgene. The bands corresponding to transgenic plants show an amplification product of 1548 bp (Fig. 1E), confirming successful integration. WT plants were used as controls for comparison with the transgenic lines to assess the outcomes of the introduced *CaAP* gene. Consequently, two transgenic lines (Nt-CaAP1 and Nt-CaAP2) were chosen for subsequent analysis. All lines exhibit comparable phenotypes (Fig. 1F), indicating the absence of obvious morphological deviations in transgenic plants.

Seed Germination Under Stress Conditions

The results showed that under control conditions, all lines (WT, Nt-CaAP1, and Nt-CaAP2) achieved 100% germination (Fig. 2). However, the transgenic lines demonstrated a slight advantage in germination speed, reaching full germination approximately one day earlier than the WT plants. This advantage became more pronounced under phosphate-deficient conditions: by the 10th day of the experiment, germination rates for Nt-CaAP1 and Nt-CaAP2 were 88% and
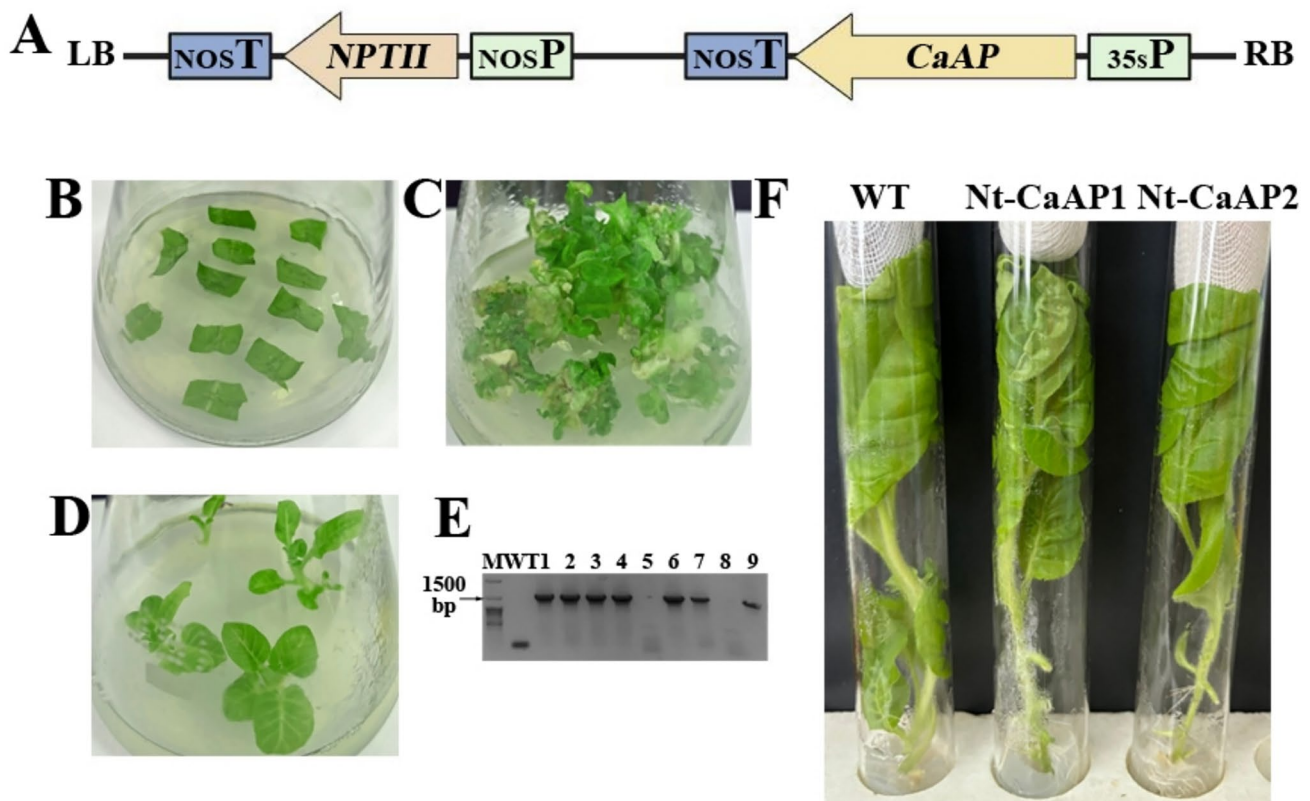
Fig. 1 Results of *Agrobacterium*-mediated genetic transformation of *N. tabacum* with the pHREAC-CaAP construct. **A** Schematic illustration of the binary vector pHREAC-CaAP, containing the 35S promoter (35SP) from cauliflower mosaic virus (CaMV), the *CaAP* gene, the selectable marker gene neomycin phosphotransferase II (*NPTII*) under the control of the nopaline synthase promoter (nosP) and terminator (nosT), as well as the right (RB) and left (LB) T-DNA borders. **B** Tobacco leaf explants following infection with *Agrobacterium tumefaciens* containing the pHREAC-CaAP construct. **C** Formation of calli and regeneration of antibiotic-resistant shoots after selection with kanamycin. **D** Elongation of regenerated shoots and induction of roots on selective medium. **E** PCR analysis confirming the integration of the *CaAP* gene in putative transgenic lines. Lane M: molecular weight marker, WT: wild-type plant, Lanes 1–9: tested putative transgenic lines. Bands corresponding to the expected 1548 bp indicate successful transformation in multiple lines. **F** Morphological comparison of WT and *CaAP*-expressing *N. tabacum*

84%, respectively, compared to only 68% for WT (Fig. 2). Under phosphate-abundant conditions, all lines exhibited high germination rates, achieving 100% germination by the 9th day (Fig. 2). Salt and osmotic stresses significantly reduced the germination rates of WT seeds (70–76%). However, lines Nt-CaAP1 and Nt-CaAP2 showed greater tolerance, with germination rates of 93–98%. Additionally, during the early stages of germination, the modified lines consistently outperformed WT plants: by the 7th day, 50% of Nt-CaAP1 and Nt-CaAP2 seeds had germinated, compared to only 25% for WT (Fig. 2). In contrast, under calcium-deficient conditions, the *CaAP*-expressing plants exhibited reduced adaptability. By the 10th day of the experiment, germination rates for Nt-CaAP1 and Nt-CaAP2 dropped to 63%, compared to 90% for WT. Furthermore, during the early stages of germination, the transgenic lines showed a pronounced lag, with germination rates approximately three times slower than WT (Fig. 2). *CaAP*-expressing lines consistently outperformed WT plants under salt and osmotic stress but showed reduced performance under calcium-deficient conditions.

Root System Development Under Abiotic Stress Conditions

Under control conditions, both Nt-CaAP1 and Nt-CaAP2 lines exhibited a slight increase in root length compared to WT. The average root lengths were 26.6 mm for Nt-CaAP1 and 26.2 mm for Nt-CaAP2, compared to 24.1 mm for WT. In phosphate-deficient environments, Nt-CaAP1 and Nt-CaAP2 exhibited root lengths 2.7-fold greater than WT (Fig. 3). Excessive phosphate levels in the medium had no effect on root growth across all tested lines, with root lengths similar to those observed under control conditions (Fig. 3). Under salt and osmotic stress conditions, the transgenic lines showed a substantial advantage in root length, exceeding

Fig. 2 A Morphological appearance of seed germination in WT and *CaAP*-expressing *N. tabacum* under abiotic stress conditions. **B** Seed germination rates. Data are presented as mean values ± standard error from three independent replicates, with a minimum of 50 seeds counted per replicate
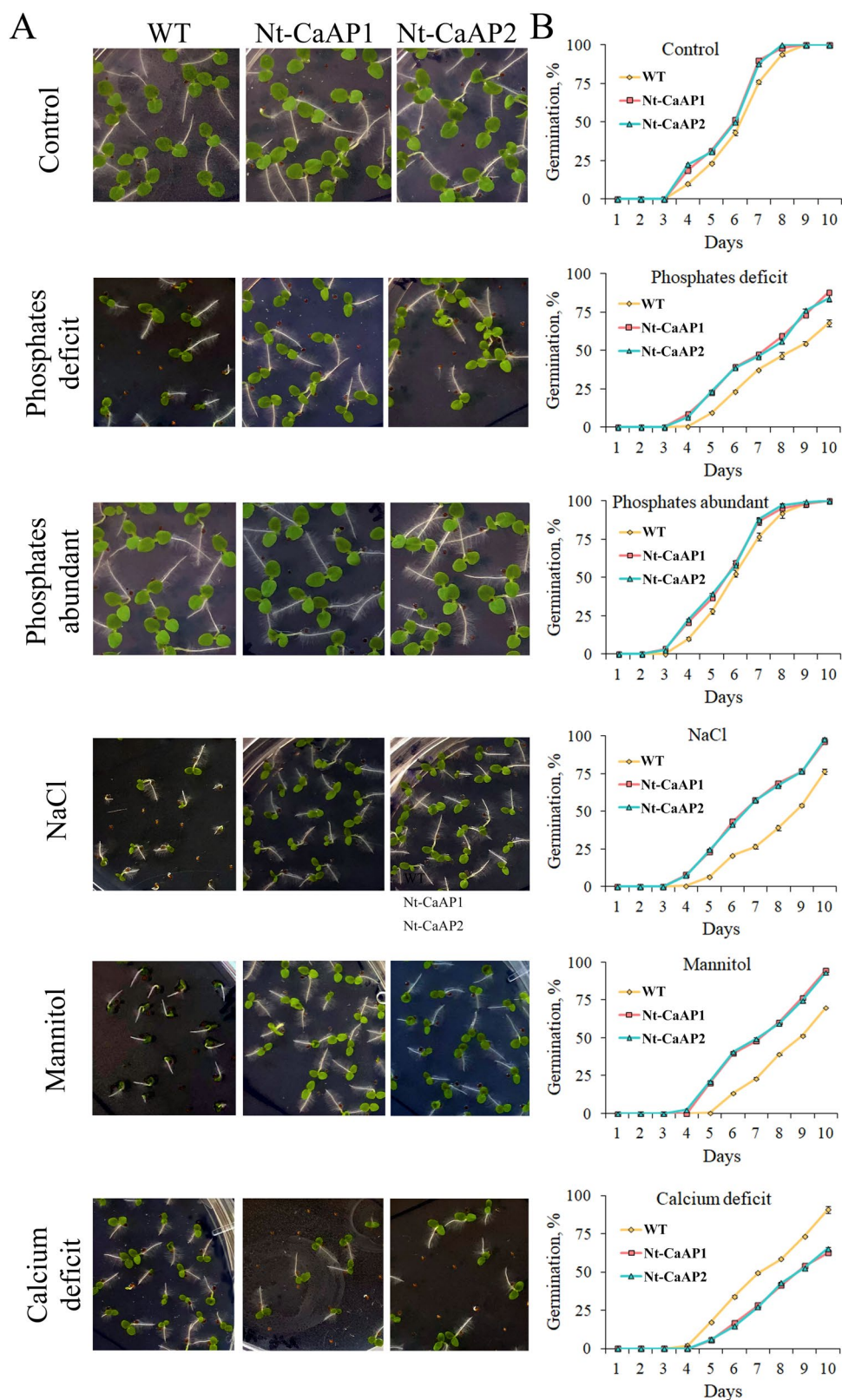
WT by factors of 1.6 and 5, respectively. However, under calcium-deficient conditions, root growth was significantly restricted in all tested lines. In this scenario, WT plants
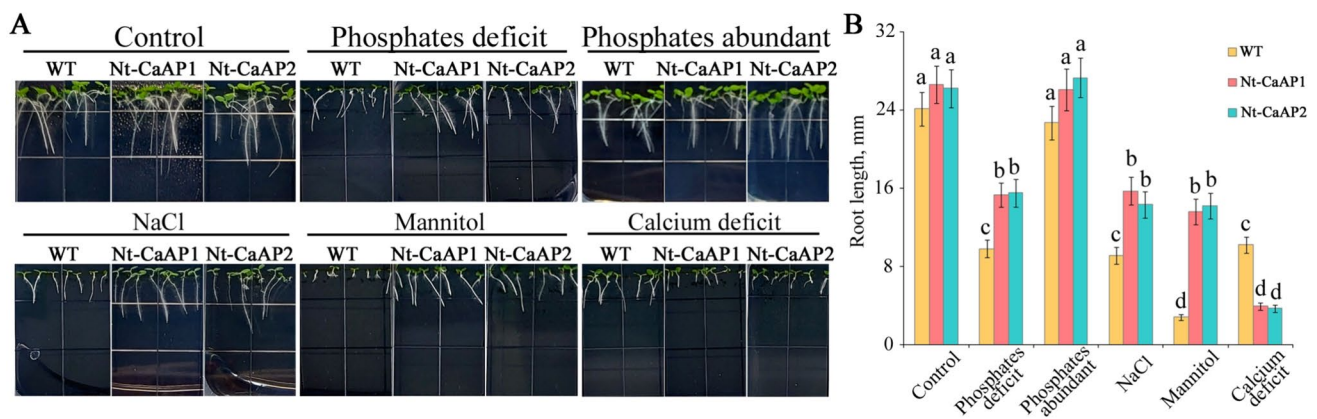
Fig. 3 Root growth of WT and *CaAP*-expressing *N. tabacum* under abiotic stress conditions. Seeds were sown in groups of 7–10 on square plates. **A** Representative images of plates were taken two weeks after sowing. **B** Statistical analysis of root growth. Data are presented as mean values ± standard error calculated from three biological replicates. Values marked with the same letter are not significantly different at $p < 0.05$, according to the LSD test

exhibited root lengths 2.7 times greater than those of the transgenic lines (Fig. 3).

Analysis of Oxidative Stress Levels, Redox Status and Polyphenol Estimation

Under control conditions, peroxidase activity was uniformly low across all tested lines, with negligible variation between WT, Nt-CaAP1, and Nt-CaAP2 (Fig. 4A). In phosphate-deficient media, peroxidase activity nearly doubled relative to control levels in all lines, yet no significant differences were observed between *CaAP*-expressing and WT plants (Fig. 4A). Excess phosphate in the growth medium did not influence peroxidase activity, which remained comparable to control values (Fig. 4A).

Under salt and osmotic stress, WT plants displayed a 2.8-fold increase in peroxidase activity, the highest levels recorded among the tested conditions and lines (Fig. 4A). Similarly, calcium-deficient conditions led to a 1.5-fold rise in peroxidase activity across all lines compared to control conditions. However, Nt-CaAP1, Nt-CaAP2 and WT plants exhibited comparable activity under calcium deficiency, with no notable differences detected (Fig. 4A).

Under control conditions, as well as in phosphate-deficient and phosphate-abundant environments, H_2O_2 content remained consistently low across all lines, ranging from 270 to 370 µmol/g fresh weight (Fig. 4B). However, exposure to salt and osmotic stress caused a dramatic fourfold increase in H_2O_2 levels compared to control conditions. WT plants accumulated approximately 1900 µmol/g fresh weight, whereas Nt-CaAP1 and Nt-CaAP2 exhibited significantly lower levels, around 1200 µmol/g fresh weight (Fig. 4B). Similarly, calcium deficiency induced a fourfold increase in H_2O_2 content in all lines compared to

control conditions, with values ranging between 900 and 1000 µmol/g fresh weight. In this scenario, no notable differences were detected between WT and the transgenic lines (Fig. 4B).

In terms of MDA content, a marker of lipid peroxidation, all lines demonstrated low levels, approximately 1 nmol/g fresh weight, under control conditions and in phosphate-abundant environments, with no significant variation between WT, Nt-CaAP1, and Nt-CaAP2 (Fig. 4C). Phosphate deficiency induced oxidative stress, doubling MDA levels across all lines compared to controls, but no differences were observed between transgenic and WT plants (Fig. 4C). Under salt and osmotic stress, MDA content increased twofold in both WT and transgenic lines compared to control conditions. However, WT plants accumulated 1.5 to 2.3 times more MDA than Nt-CaAP1 and Nt-CaAP2 under these stress conditions (Fig. 4C). Conversely, in calcium-deficient conditions, transgenic lines were more sensitive, showing MDA levels 1.5 times higher than those in WT plants (Fig. 4C).

The IC_{50} values for DPPH radical scavenging activity remained relatively low under control conditions and phosphate-abundant environments, ranging from 78 to 89 µg/mL across all lines (Fig. 4D). In contrast, phosphate deficiency, calcium deficiency, and salt and osmotic stress significantly increased IC_{50} values by approximately 1.5 times compared to control conditions (Fig. 4D). No differences in IC_{50} values were observed between WT and *CaAP*-expressing lines under phosphate-deficient conditions. However, under salt and osmotic stress, WT plants showed IC_{50} values 1.3 times higher than those of Nt-CaAP1 and Nt-CaAP2. Under calcium-deficient conditions, the trend was reversed, with transgenic lines exhibiting IC_{50} values 1.3 times greater than those of WT plants (Fig. 4D).
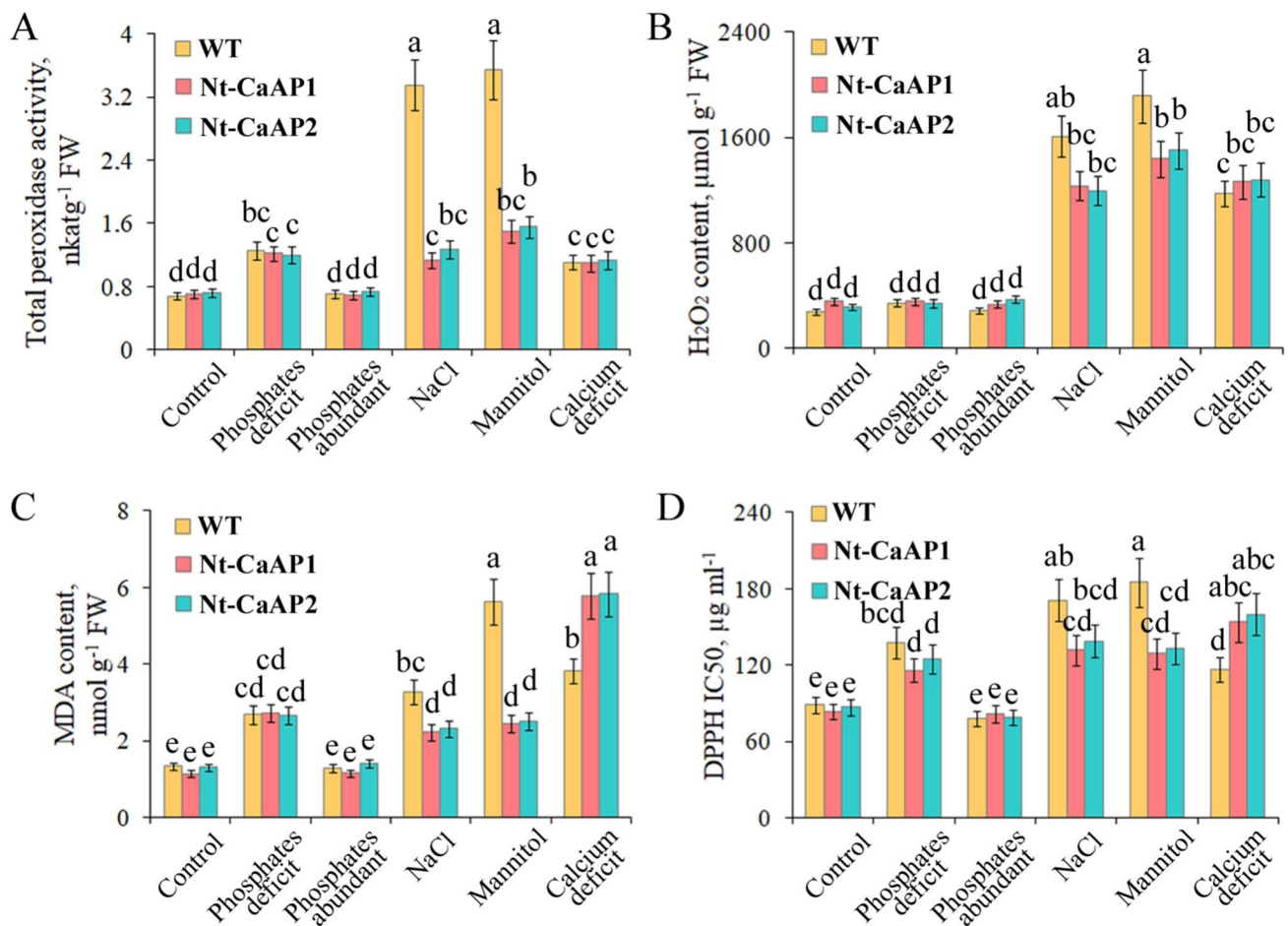
Fig. 4 Impact of abiotic stresses on the redox status in WT and *CaAP*-expressing *N. tabacum*. **A** Total peroxidase activity; **B** hydrogen peroxide accumulation levels; **C** MDA content; **D** antioxidant activity measured by the DPPH assay. Data are presented as mean values ± standard error. Values marked with the same letter are not significantly different at $p < 0.05$, according to the LSD test

Table 1 Polyphenol and proline content estimation

Samples	TPC (µg GAE/g)	TFC (µg QE/g)	Proline content (µg/g)
WT	6010 ± 297	260 ± 9	17.165 ± 0.645
Nt-CaAP1	9540 ± 425*	570 ± 21*	57.316 ± 2.107*
Nt-CaAP2	9820 ± 495*	490 ± 22*	59.105 ± 2.282*

Data are presented as mean values ± standard error. Values in rows marked with an asterisk (*) differ significantly at $p < 0.05$, according to the LSD test

Total phenolic content (TPC) expressed as gallic acid equivalents (GAE) showed markedly higher levels in both transgenic lines compared to WT (Table 1). Specifically, Nt-CaAP1 and Nt-CaAP2 exhibited 1.6-fold increase over the WT value of 6010 µg GAE/g. Similarly, total flavonoid content (TFC) measured as quercetin equivalents (QE) demonstrated significant enhancement in the *CaAP*-expressing plants (Table 1). The WT samples showed a baseline TFC

of 260 µg QE/g. while Nt-CaAP1 and Nt-CaAP2 displayed in 2-times elevated. Perhaps the most striking difference was observed in proline content (Table 1), where both transgenic lines showed dramatic elevation compared to WT. While WT samples contained 17.2 µg/g fresh weight of proline Nt-CaAP1 and Nt-CaAP2 exhibited levels of 57.3 and 59.1 µg/g fresh weight, respectively, representing a more than 3.3-fold increase.

Physiological Characteristics

The MSI serves as an indicator of cellular membrane integrity, with higher MSI values reflecting better membrane stability and resilience to stress-induced damage. Under control conditions and in environments with excess phosphate, all lines exhibited high MSI values, reaching approximately 90% (Fig. 5A). However, phosphate deficiency led to a decline in membrane stability across all lines, with MSI values dropping to 70% compared to control conditions. Salt
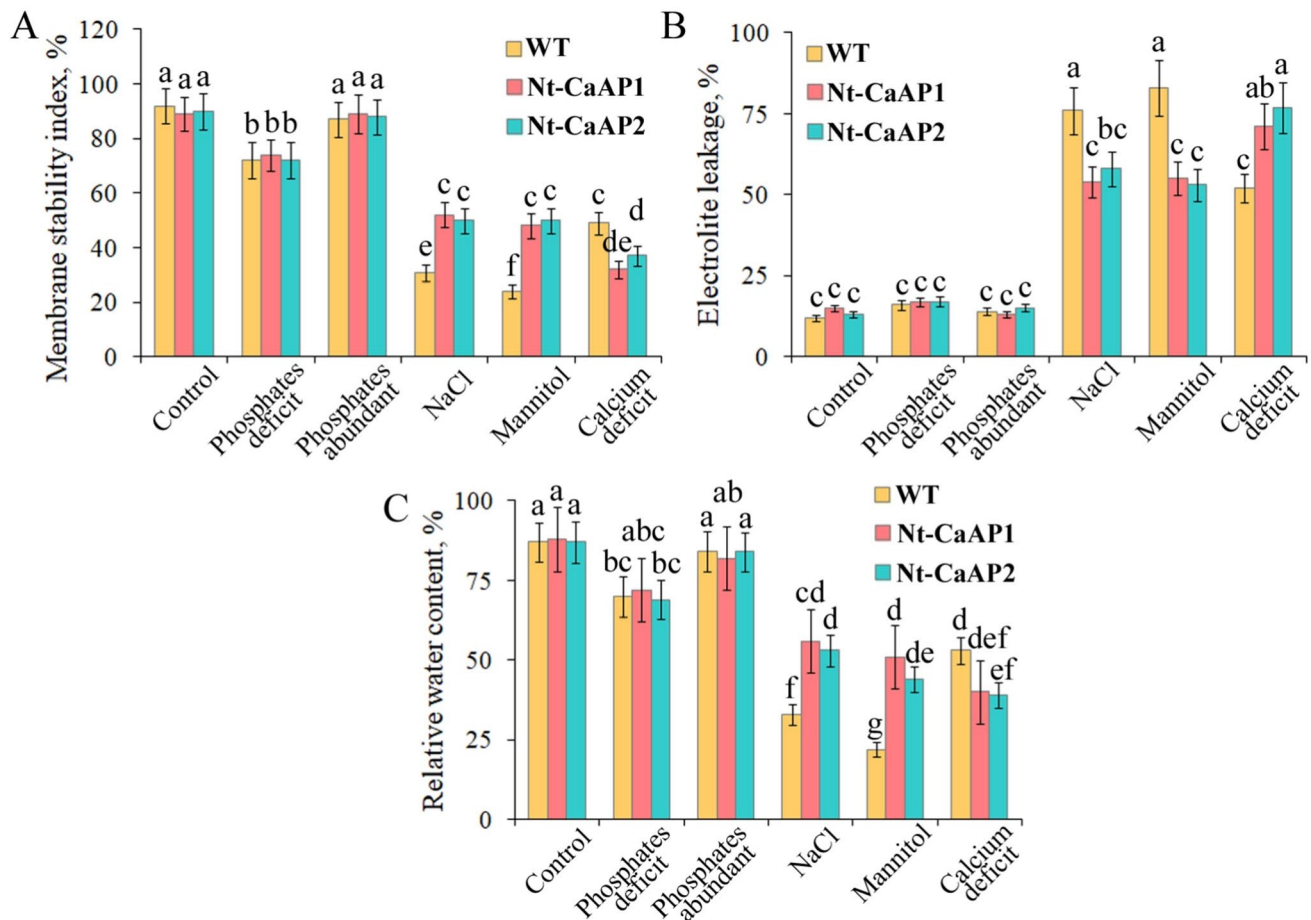
Fig. 5 Analysis of physiological parameters in WT and *CaAP*-expressing *N. tabacum*. **A** MSI; **B** electrolyte leakage; **C** RWC in leaves. Data are presented as mean values ± standard error. Values marked with the same letter are not significantly different at $p < 0.05$, according to the LSD test

and osmotic stresses significantly impaired membrane integrity. In WT plants, MSI values decreased by 3–4 times relative to control conditions and were 1.6–2.0 times lower than those observed in Nt-CaAP1 and Nt-CaAP2 under the same stress conditions (Fig. 5A). A similar trend was observed under calcium-deficient conditions, where MSI substantially declined in all lines. However, in this case, WT plants outperformed the transgenic lines, maintaining higher MSI values (Fig. 5A).

Figure 5B presents the percentage of electrolyte leakage, an indicator of cell membrane damage, where higher percentages reflect more severe structural disruptions. Under control conditions, as well as under phosphate-deficient and phosphate-abundant conditions, electrolyte leakage remained low and showed minimal variation between lines. However, salt and osmotic stresses, along with calcium deficiency, significantly increased electrolyte leakage, exceeding control levels by 4–7 times (Fig. 5B). Nt-CaAP1 and Nt-CaAP2 demonstrated

enhanced tolerance to salt and osmotic stresses, exhibiting electrolyte leakage levels approximately 1.5 times lower than those of WT. In contrast, under calcium-deficient conditions, the transgenic lines showed higher electrolyte leakage, reaching 71–75% (Fig. 5B). Relative water content (RWC) reflects the ability of plant tissues to retain water, with higher RWC percentages indicating better hydration and a balanced water status. Under control conditions, as well as under phosphate-deficient and phosphate-abundant conditions, RWC levels remained relatively high across all lines, ranging from 70–88% (Fig. 5C). Under salt and osmotic stresses, WT plants experienced a significant reduction in RWC, with levels dropping to 22–33%. In contrast, *CaAP*-expressing lines maintained higher hydration levels, retaining over 50% of water content (Fig. 5C). In calcium-deficient conditions, water retention capacity decreased in all lines, with RWC values reduced to approximately 50% of the levels observed under control conditions (Fig. 5C).
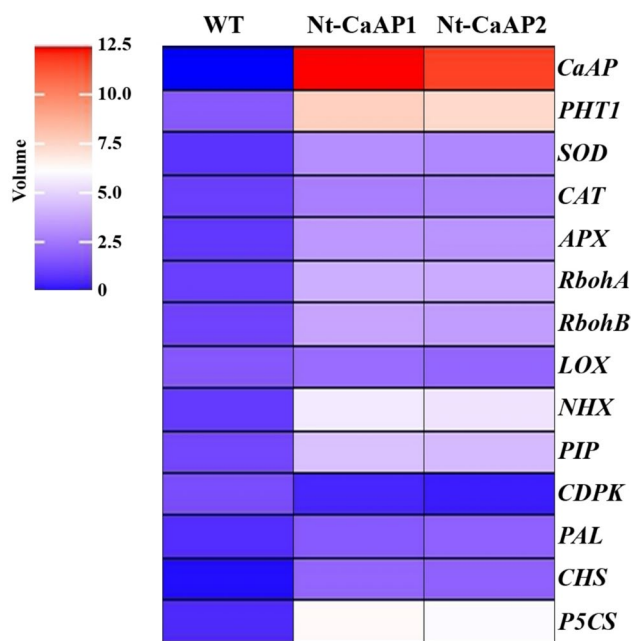
Fig. 6 Expression analysis of the *CaAP* transgene and genes involved in antioxidant defense (*SOD*, *CAT*, *APX*), prooxidant pathways (*RbohA*, *RbohB*), lipid metabolism (*LOX*), ion transport (*NHX*), water transport (*PIP*), calcium-dependent protein kinase activity (*CDPK*), phenolic and flavonoid biosynthesis (*PAL*, *CHS*), and proline biosynthesis (*P5CS*) in WT and *CaAP*-expressing *N. tabacum*

Molecular Analysis of Biological Functions of *CaAP* Gene in Transgenic Tobacco

To assess the impact of *CaAP* gene expression in tobacco, we performed qPCR analysis to quantify *CaAP* transcript levels (Fig. 6). The analysis revealed significant differences in gene expression between the WT and transgenic lines. High levels of *CaAP* gene expression were observed in both lines, whereas no expression was detected in WT plants. These findings confirm the successful transformation and strong activation of the transgene in the transgenic lines.

Among the analyzed genes, *PHT1* exhibited a pronounced upregulation, with mRNA levels increasing more than fourfold in both Nt-CaAP1 and Nt-CaAP2 compared to WT. Genes encoding antioxidant enzymes showed moderate increases in expression in the transgenic lines. *SOD* transcripts rose by 3.75- to fourfold, *CAT* expression increased 2.5-fold, and *APX* expression was elevated more than 3.8-fold relative to WT. ROS signaling-related genes, *RbohA* and *RbohB*, demonstrated similar transcript increases of approximately threefold in the *CaAP*-expressing plants. The *LOX* expression showed minimal variation between WT and transgenic lines. Significant changes were observed in the expression of genes related to ion homeostasis and transport. *NHX* transcripts increased markedly in Nt-CaAP1 and Nt-CaAP2, reaching 5.8-fold above WT levels, while *PIP*

expression exhibited a 3.5-fold enhancement. In contrast, *CDPK* mRNA levels decreased, showing a fourfold reduction in the transgenic lines. Genes associated with secondary metabolism exhibited notable increases in expression in the transgenic plants. *PAL* showed a 2.9-fold enhancement, while *CHS* expression increased by more than 15-fold compared to WT. Additionally, the stress-responsive gene *P5CS* demonstrated a dramatic increase, with mRNA levels rising tenfold in Nt-CaAP1 and Nt-CaAP2 relative to WT.

Discussion

This study marks the first instance of the *in planta* heterologous expression of the *CaAP* gene from the marine bacterium *C. amphilecti*. The experiment was designed to investigate whether endogenous expression of the gene could improve plant tolerance to abiotic stress factors. *CaAP*-expressing tobacco seeds demonstrated enhanced germination rates under conditions of phosphate deficiency, salinity, and osmotic stress, suggesting that the expression of *CaAP* alleviates the detrimental effects of these stressors and supports seedling establishment. However, this advantageous effect was absent in calcium-deficient media, indicating a specific limitation of this transgenic approach in such conditions.

Phosphate deficiency has a multifaceted impact on plant development (Rouached et al. 2011). While it impairs cellular energy production by reducing ATP availability, thereby inhibiting cell division and growth, it simultaneously induces adaptive responses, such as resource reallocation to root development (Péret et al. 2011). This adaptation increases the root surface area, facilitating improved phosphate uptake. In Nt-CaAP1 and Nt-CaAP2 plants, such resource redistribution was significantly enhanced, likely due to the functional activity of the *CaAP* transgene, which strengthens root system adaptation to phosphorus scarcity. Previous studies have frequently reported elevated acid phosphatase activity in plant tissues under phosphorus-deficient conditions. For example, increased root development and exudation of acid phosphatase have been observed under phosphate deficiency in various maize genotypes (Duff et al. 1994). Similarly, the secretion of acid phosphatase by roots in phosphorus-deficient conditions was found to vary across plant species, with particularly high activity in lupin and tomato, moderate activity in soybean and sugar beet, and low activity in wheat and azuki bean (Tadano et al. 1993). Recent work with biofilmed-PGPR (Plant Growth-Promoting Rhizobacteria) demonstrated enhanced phosphate solubilization and nutrient uptake in rice, contributing to improved growth under abiotic stress conditions (Bright et al. 2025). These findings collectively underscore the importance of phosphatase activity and root system adaptation in plant responses to

phosphate deficiency, which was further amplified in the studied transgenic tobacco lines expressing the *CaAP* gene.

We hypothesized that heterologous expression of *CaAP* in tobacco plants would enhance their adaptation to phosphate-deficient conditions. Indeed, under complete phosphate deprivation, *CaAP*-expressing lines exhibited higher seed germination rates and more developed root systems compared to wild-type plants. These advantages may stem from more efficient redistribution of internal phosphorus reserves and the maintenance of critical energy-dependent processes during early growth stages. Additionally, the enhanced root development observed in the transgenic lines may reflect activation of adaptive mechanisms aimed at improving nutrient acquisition, even in the absence of external phosphate sources. Comparative evidence from rice supports the utility of bacterial phosphatases in nutrient-stress adaptation. For example, Ram et al. (2019) showed that transgenic rice plants overexpressing phoA, a bacterial APs, displayed improved root and shoot growth, increased total biomass, and enhanced utilization of phosphite (Phi) as a phosphorus source. Although our findings align with these results, it additionallyrevealed a novel calcium-dependent sensitivity. This distinction highlights both the potential and limitations of marine bacterial APs in plant biotechnology, and suggests that cofactor dependencies must be considered when transferring microbial genes into crop systems. Overall, these findings suggest that under phosphate-deficient conditions, AP exhibits function similar to those under phosphate-rich conditions. These functions include restricting pigment biosynthesis, photosynthesis, fatty acid synthesis, and cell division. Such regulatory roles are essential for maintaining metabolic balance and preventing premature cell division, thereby supporting overall plant stress tolerance and development (Zhang et al. 2021).

Salt and osmotic stresses are known to impose severe oxidative stress on plants (Solis et al. 2022). Under these conditions, *CaAP* expression appeared to play an auxiliary role in phosphate redistribution and energy metabolism maintenance, enabling transgenic plants to better tolerate these stresses. This enhanced stress tolerance was reflected in improved seeds germination and greater root length in Nt-CaAP1 and Nt-CaAP2 lines compared to WT, correlating with better regulation of redox homeostasis. Additionally, *CaAP* expression in transgenic lines enhanced antioxidant capacity and improved stress tolerance associated with reduced peroxidase activity, lower H_2O_2 accumulation, and decreased malondialdehyde (MDA) levels. Furthermore, the IC_{50} value for DPPH scavenging activity was lower in both lines compared to WT under salt and osmotic stress. These effects contributed to improved membrane stability, reduced structural damage, minimized electrolyte leakage, and better water retention in leaves, collectively enhancing plant resilience to these stress conditions. Previous research has shown that transgenic rice and *Arabidopsis* plants expressing ion transport-regulating genes, such as *NHX1*, exhibit enhanced tolerance to abiotic stress. This improvement is attributed to the gene's role in maintaining ionic homeostasis and mitigating oxidative stress under salt and osmotic stress conditions (Solis et al. 2022; Kumar et al. 2017). The stress tolerance observed in *CaAP*-expressing lines may, in part, be attributed to improved phosphorus metabolism mediated by the phosphatase activity of CaAP. By hydrolyzing organic phosphate compounds and enhancing local phosphate availability, CaAP likely supports sustained ATP synthesis under stress conditions. This, in turn, could fuel energy-intensive protective mechanisms such as antioxidant enzyme activity and membrane repair. Enhanced ATP levels may also facilitate efficient ROS detoxification through ATP-dependent antioxidant pathways, contributing to the lower levels of lipid peroxidation and improved membrane stability observed in transgenic plants.

This study intriguingly revealed that plants expressing *CaAP* exhibited heightened sensitivity to calcium deficiency compared to WT plants. Calcium is a vital secondary messenger that regulates plant responses to various abiotic and biotic stresses. The cytoplasmic concentration of calcium directly modulates the activity of calcium-dependent enzymes and governs the transcription of stress-responsive genes. Many enzymes, including phosphatases, rely on calcium as a cofactor, with calcium ions binding to specific sites to enhance their catalytic efficiency. Calcium deficiency disrupts the activity of antioxidant enzymes, such as phosphatases, resulting in increased ROS levels and subsequent cellular damage (Knight 2000). Previous studies have emphasized the critical role of calcium in regulating phosphate metabolism, particularly through the activity of phosphatases involved in recycling organic phosphate compounds. This regulation enables plants to adapt to phosphate-deficient conditions, further demonstrating the essential interplay between calcium and phosphorus in plant nutrient management (Jing et al. 2024). The findings of this study underscore the interconnected roles of calcium and phosphate in plant stress tolerance and highlight the potential of *CaAP* to enhance resilience to specific abiotic stresses. Beyond its direct catalytic dependence on calcium, the overexpression of *CaAP* may have indirectly affected calcium-dependent signaling and homeostasis in the transgenic lines. The heightened demand for Ca^{2+} by the heterologous enzyme could disrupt the availability of free calcium for native signaling components, such as CDPKs, calmodulins, and membrane-associated transporters. This shift may impair critical calcium-mediated responses to stress, including membrane stabilization, ROS detoxification, and transcriptional regulation of stress-responsive genes. The observed downregulation of *CDPK* expression in the transgenic plants supports this hypothesis and suggests that the

calcium deficiency phenotype is not solely enzymatic but also linked to broader signaling imbalances. However, they also reveal the limitations of transgenic strategies under calcium-deficient conditions, where disrupted calcium signaling compromises the plant's ability to mitigate oxidative stress.

The integration and expression of the *CaAP* gene in tobacco lines resulted in significant alterations in secondary metabolite profiles and stress-related compounds, suggesting a broader regulatory role for this enzyme than previously recognized. The marked elevation of TPC in both Nt-CaAP1 and Nt-CaAP2 lines indicates that *CaAP* likely modulates key enzymes in the phenylpropanoid pathway. This enhancement of phenolic compounds correlates to improved stresses tolerance, as phenolics are well-documented to play crucial roles in plant defense mechanisms and antioxidant responses (Dixon and Paiva 1995). The parallel increase in total flavonoid content in transgenic lines, further supports the hypothesis that *CaAP* involved regulator of secondary metabolism. Flavonoids, as a subset of phenolic compounds, are particularly important for their diverse roles in plant defense, UV protection, and signaling (Winkel-Shirley 2001). Perhaps the most striking observation was the dramatic accumulation of proline in both Nt-CaAP lines. This substantial increase in proline content is particularly noteworthy, as proline serves multiple functions in plant stress responses, including osmolyte balance, protein protection, and ROS scavenging (Szabados and Savouré 2010). The coordinated elevation of phenolics, flavonoids and proline content suggests that heterologous expression of *CaAP* may indirectly regulate metabolic changes through protein dephosphorylation-mediated signaling cascades. Recently, rhizosphere engineering using biocontrol agents has been shown to enrich soil microbial diversity and effectively suppress root-knot nematodes, in part through the modulation of plant immune responses and beneficial microbiome restructuring (Vinothini et al. 2024). The phosphatase activity could target transcription factors that control secondary metabolism, potentially removing inhibitory phosphorylation marks and enabling their activation. This would explain the coordinated upregulation of multiple metabolic pathways observed in our study.

Transcriptional profiling of Nt-CaAP transgenic lines revealed complex changes in the expression of genes involved in various metabolic and signaling pathways, indicating a broad spectrum of regulatory influence of *CaAP* phosphatase. Transcriptional profiling of *CaAP*-expressing plants revealed complex changes in gene expression across various metabolic and signaling pathways. The significant upregulation of *PHT1* in both transgenic lines indicates enhanced phosphate transport, which may be linked to altered phosphate homeostasis resulting from *CaAP* phosphatase activity. This modification likely influences the overall mineral metabolism of plants and may contribute to their

improved growth and development (Wang et al. 2017; Yang et al. 2024). The coordinated upregulation of antioxidant enzymes (*SOD*, *CAT*, and *APX*) suggests enhancement of the antioxidant system in transgenic lines. Elevated transcript levels of these enzymes indicate a more efficient ROS detoxification system (Mittler et al. 2004; Choudhury et al. 2017). The parallel increase in *RbohA* and *RbohB* expression suggests enhanced ROS-mediated signaling, which may play a crucial role in regulating plant defense responses (Yan et al. 2006; Torres and Dangl 2005). The absence of significant changes in *LOX* expression suggests that the lipoxygenase pathway is not a primary target of *CaAP* regulation (Wasternack and Feussner 2018). Particularly noteworthy are the changes in ion homeostasis-related gene expression. Significant upregulation of *NHX* and *PIP* transcripts indicates substantial modification of ion and water transport systems. This may contribute to improved osmoregulation and enhanced abiotic stress tolerance (Apse and Blumwald 2007; Maurel et al. 2015). Interestingly, *CDPK* expression showed a fourfold decrease, which may reflect a compensatory mechanism in response to altered phosphatase activity (Schulz et al. 2013; Yan et al. 2006). The dramatic increase in secondary metabolism genes, such as *CHS* and *PAL*, aligns with the observed elevation in phenolic compounds and flavonoids in transgenic lines. This suggests that *CaAP* may act as a regulator of phenylpropanoid pathway, possibly through dephosphorylation cascades of key transcription factors (Dixon and Paiva 1995). This pathway is known to produce a wide range of secondary metabolites that function in ROS scavenging, UV protection, and stress signaling (Dixon and Paiva 1995), which may explain the enhanced oxidative stress tolerance observed in transgenic lines. Given the phenylpropanoid pathway's role in synthesizing structural barriers (e.g., lignin precursors), its activation might also contribute to enhanced cell wall reinforcement, providing physical protection under osmotic and salt stress. The increase in *P5CS* expression correlates well with elevated proline content in transgenic lines and confirms a direct link between *CaAP* activity and osmoprotectant biosynthesis. This may be one of the key mechanisms through which *CaAP* influences plant stress tolerance, though this aspect requires further detailed investigation. Thus, the observed improvements in salinity and osmotic stress tolerance suggest that *CaAP* has potential as a biotechnological tool to enhance crop tolerance in saline environments, provided that sufficient calcium is available to support enzymatic activity.

Conclusion

In this study, we demonstrated that heterologous expression of the *CaAP* gene from the marine bacterium *C. amphilecti* in tobacco enhances plant tolerance to abiotic stresses,

including salinity and osmotic stress. The improved performance of transgenic lines was associated with higher antioxidant enzyme activity, reduced ROS accumulation, increased phenolic and flavonoid content, and altered expression of key stress-responsive genes. However, these benefits did not extend to phosphate-deficient conditions, likely due to limitations CaAP in roots and its calcium dependency. Importantly, *CaAP*-expressing plants exhibited sensitivity to calcium deficiency, highlighting a previously underexplored metabolic trade-off. While these findings support the potential of *CaAP* as a stress-tolerance gene for biotechnological applications, all experiments were conducted under controlled in vitro conditions. Future greenhouse and field studies are essential to validate the observed traits and assess the suitability of this approach for sustainable crop improvement, particularly in saline environments with adequate calcium availability.

Declarations

References

Adedibu PA, Noskova YA, Yugay YA, Ovsiannikova DM, Vasyutkina E, Kudinova OD, Grigorchuk V, Shkryl Y, Tekutyeva LA, Balabanova L (2024) Expression and characterization of alkaline phosphatase from *Cobetia amphilecti* KMM 296 in transiently transformed tobacco leaves and transgenic calli. Plants (Basel) 13:3570. https://doi.org/10.3390/plants13243570

Apse MP, Blumwald E (2007) Na^+ transport in plants. FEBS Lett 581:2247–2254. https://doi.org/10.1016/j.febslet.2007.04.014

Balabanova L, Nedashkovskaya O, Podvolotskaya A, Slepchenko L, Golotin V, Belik A, Shevchenko L, Son O, Rasskazov V (2016) Data supporting functional diversity of the marine bacterium *Cobetia amphilecti* KMM 296. Data Brief 8:726–732. https://doi.org/10.1016/j.dib.2016.06.034

Balabanova L, Seitkalieva A, Yugay Y, Rusapetova T, Slepchenko L, Podvolotskaya A, Yatsunskaya M, Vasyutkina E, Son O, Tekutyeva L, Shkryl Y (2022) Engineered fungus *Thermothelomyces thermophilus* producing plant storage proteins. J Fungi 8:119. https://doi.org/10.3390/jof8020119

Bates LS, Waldren R, Teare I (1973) Rapid determination of free proline for water-stress studies. Plant Soil 39:205–207. https://doi.org/10.1007/BF00018060

Blum A, Ebercon A (1981) Cell membrane stability as a measure of drought and heat tolerance in *Triticum* (*wheat*). Crop Sci 21:43–47. https://doi.org/10.2135/cropsci1981.0011183X002100010013x

Bright JP, Maheshwari HS, Thangappan S, Perveen K, Bukhari NA, Mitra D, Sayyed R, Mastinu A (2025) Biofilmed-PGPR: next-generation bioinoculant for plant growth promotion in rice under changing climate. Rice Sci 32:94–106. https://doi.org/10.1016/j.rsci.2024.08.008

Buege JA, Aust SD (1978) Microsomal lipid peroxidation. Methods Enzymol 52:302–310. https://doi.org/10.1016/s0076-6879(78)52032-6

Choudhury FK, Rivero RM, Blumwald E, Mittler R (2017) Reactive oxygen species, abiotic stress and stress combination. Plant J 90:856–867. https://doi.org/10.1111/tpj.13299

Coleman JE (1992) Structure and mechanism of alkaline phosphatase. Annu Rev Biophys Biomol Struct 21:441–483. https://doi.org/10.1146/annurev.bb.21.060192.002301

Degtyarenko AI, Grigorchuk V, Sorokina M, Yugay Y, Fialko A, Grishchenko O, Vasyutkina E, Kudinova O, Tsydeneshieva ZL, Bulgakov V, Shkryl Y (2024) Expression of the *LlBANMT* gene from *sea lavender* leads to the accumulation of β-alanine betaine and enhanced stress resilience in transgenic tobacco plants. J Plant Growth Regul. https://doi.org/10.1007/s00344-024-11526-1

Dixon RA, Paiva NL (1995) Stress-induced phenylpropanoid metabolism. Plant Cell 7:1085–1097. https://doi.org/10.1105/tpc.7.7.1085

Duff SMG, Sarath G, Plaxton WC (1994) The role of acid phosphatases in plant phosphorus metabolism. Physiol Plant 90:791–800. https://doi.org/10.1111/j.1399-3054.1994.tb02539.x

Ferrer MA, Calderón AA, Muñoz R, Ros Barceló A (1990) 4-methoxy-α-naphthol as a specific substrate for kinetic, zymographic and cytochemical studies on plant peroxidase activities. Phytochem Anal 1:63–69. https://doi.org/10.1002/pca.2800010203

Gerke J (2024) Improving phosphate acquisition from soil via higher plants while approaching peak phosphorus worldwide: a critical review of current concepts and misconceptions. Plants 13:3478. https://doi.org/10.3390/plants13243478

Hood EE, Gelvin SB, Melchers LS, Hoekema A (1993) New *Agrobacterium* helper plasmids for gene transfer to plants. Transgenic Res 2:208–218. https://doi.org/10.1007/BF01977351

Huang W, Ratkowsky DA, Hui C, Wang P, Su J, Shi P (2019) Leaf fresh weight versus dry weight: which is better for describing the scaling relationship between leaf biomass and leaf area for broad-leaved plants? Forests 10:256. https://doi.org/10.3390/f10030256

Jing T, Li J, He Y, Shankar A, Saxena A, Tiwari A, Maturi K, Solanki MK, Singh V, Eissa M, Ding Z, Xie J, Awasthi MK (2024) Role of calcium nutrition in plant physiology: advances in research and insights into acidic soil conditions – a comprehensive review. Plant Physiol Biochem. https://doi.org/10.1016/j.plaphy.2024.108602

Junglee S, Urban L, Sallanon H, Lopez-Lauri F (2014) Optimized assay for hydrogen peroxide determination in plant tissue using potassium iodide. Am J Anal Chem 5:730–736. https://doi.org/10.4236/ajac.2014.511081

Khan F, Siddique AB, Shabala S, Zhou M, Zhao C (2023) Phosphorus plays key roles in regulating plants' physiological responses to abiotic stresses. Plants 12:2861. https://doi.org/10.3390/plants12152861

Knight H (2000) Calcium signaling during abiotic stress in plants. Int Rev Cytol 195:269–324. https://doi.org/10.1016/s0074-7696(08)62707-2

Kumar S, Kalita A, Srivastava R, Sahoo L (2017) Co-expression of *Arabidopsis NHX1* and *bar* improves the tolerance to salinity, oxidative stress, and herbicide in transgenic mungbean. Front Plant Sci 8:1896. https://doi.org/10.3389/fpls.2017.01896

Lambers H, Hayes PE, Laliberté E, Teste FP (2023) Phosphorus acquisition strategies and adaptations in plants. Plants 12:2861. https://doi.org/10.3390/plants12152861

Leubner-Metzger G, Frundt C, Vogeli-Lange R, Meins F Jr (1995) Class I β-1,3-glucanases in the endosperm of *tobacco* during germination. Plant Physiol 109:751–759. https://doi.org/10.1104/pp.109.3.751

Lindsey BE 3rd, Rivero L, Calhoun CS, Grotewold E, Brkljacic J (2017) Standardized method for high-throughput sterilization of *Arabidopsis* seeds. J vis Exp 128:56587. https://doi.org/10.3791/56587

Makris K, Mousa C, Cavalier E (2023) Alkaline phosphatases: biochemistry, functions, and measurement. Calcif Tissue Int 112:233–242. https://doi.org/10.1007/s00223-022-01048-x

Maurel C, Boursiac Y, Luu DT, Santoni V, Shahzad Z, Verdoucq L (2015) Aquaporins in plants. Physiol Rev 95:1321–1358. https://doi.org/10.1152/physrev.00008.2015

Mittler R, Vanderauwera S, Gollery M, Van Breusegem F (2004) Reactive oxygen gene network of plants. Trends Plant Sci 9:490–498. https://doi.org/10.1016/j.tplants.2004.08.009

Onwueme IC (1979) Rapid, plant-conserving estimation of heat tolerance in plants. J Agric Sci 92:527–535. https://doi.org/10.1017/S0021859600053764

Peng D, Zahid HF, Ajlouni S, Dunshea F, Suleria H (2019) LC-ESI-QTOF/MS profiling of Australian mango peel by-product polyphenols and their potential antioxidant activities. Processes 7:764. https://doi.org/10.3390/pr7100764

Péret B, Clément M, Nussaume L, Desnos T (2011) Root developmental adaptation to phosphate starvation: better safe than sorry. Trends Plant Sci 16:442–450. https://doi.org/10.1016/j.tplants.2011.05.006

Ram B, Fartyal D, Sheri V, Varakumar P, Borphukan B, James D, Yadav R, Bhatt A, Agrawal P, Achary VMM, Reddy MK (2019) Characterization of *phoA*, a bacterial alkaline phosphatase for *Phi* use efficiency in rice plant. Front Plant Sci 10:37. https://doi.org/10.3389/fpls.2019.00037

Rouached H, Stefanovic A, Secco D, Bulak Arpat A, Gout E, Bligny R, Poirier Y (2011) Uncoupling phosphate deficiency from its major effects on growth and transcriptome via *PHO1* expression in *Arabidopsis*. Plant J 65:557–570. https://doi.org/10.1111/j.1365-313X.2010.04442.x

Schulz P, Herde M, Romeis T (2013) Calcium-dependent protein kinases: hubs in plant stress signaling and development. Plant Physiol 163:523–530. https://doi.org/10.1104/pp.113.222539

Shkryl Y, Yugay Y, Vasyutkina E, Chukhlomina E, Rusapetova T, Bulgakov V (2022) The *RolB/RolC* homolog from sweet potato promotes early flowering and triggers premature leaf senescence in transgenic *Arabidopsis thaliana* plants. Plant Physiol Biochem 193:50–60. https://doi.org/10.1016/j.plaphy.2022.10.018

Shkryl YN, Tchernoded GK, Yugay YA, Grigorchuk VP, Sorokina MR, Gorpenchenko TY, Kudinova OD, Degtyarenko AI, Onishchenko MS, Shved NA, Kumeiko VV, Bulgakov VP (2023) Enhanced production of nitrogenated metabolites with anticancer potential in *Aristolochia manshuriensis* hairy root cultures. Int J Mol Sci 24:11240. https://doi.org/10.3390/ijms241411240

Singleton VL, Orthofer R, Lamuela-Raventós RM (1999) Analysis of total phenols and other oxidation substrates and antioxidants by means of Folin-Ciocalteu reagent. Methods Enzymol 299:152–178. https://doi.org/10.1016/S0076-6879(99)99017-1

Solis CA, Yong MT, Zhou M, Venkataraman G, Shabala L, Holford P, Shabala S, Chen ZH (2022) Evolutionary significance of *NHX* family and *NHX1* in salinity stress adaptation in the genus *Oryza*. Int J Mol Sci 23:2092. https://doi.org/10.3390/ijms23042092

Szabados L, Savouré A (2010) *Proline*: a multifunctional amino acid. Trends Plant Sci 15:89–97. https://doi.org/10.1016/j.tplants.2009.11.009

Tadano T, Ozawa K, Sakai H, Osaki M, Matsui H (1993) Secretion of acid phosphatase by the roots of crop plants under phosphorus-deficient conditions and some properties of the enzyme secreted by *lupin* roots. Plant Soil 155(1):95–98. https://doi.org/10.1007/BF00024992

Torres MA, Dangl JL (2005) Functions of the respiratory burst oxidase in biotic interactions, abiotic stress and development. Curr Opin Plant Biol 8:397–403. https://doi.org/10.1016/j.pbi.2005.05.014

Vinothini K, Nakkeeran S, Saranya N, Jothi P, Richard JI, Perveen K, Bukhari NA, Glick BR, Sayyed RZ, Mastinu A (2024) Rhizosphere engineering of biocontrol agents enriches soil microbial diversity and effectively controls root-knot nematodes. Microb Ecol 87:120. https://doi.org/10.1007/s00248-024-02435-7

Wang D, Lv S, Jiang P, Li Y (2017) Roles, regulation, and agricultural application of plant phosphate transporters. Front Plant Sci 8:817. https://doi.org/10.3389/fpls.2017.00817

Wasternack C, Feussner I (2018) The oxylipin pathways: biochemistry and function. Annu Rev Plant Biol 69:363–386. https://doi.org/10.1146/annurev-arplant-042817-040440

White Philip R (1954) The cultivation of animal and plant cells. Bioscience 4:13. https://doi.org/10.1093/aibsbulletin/4.3.13-d

Winkel-Shirley B (2001) Flavonoid biosynthesis. A colorful model for genetics, biochemistry, cell biology, and biotechnology. Plant Physiol 126:485–493. https://doi.org/10.1104/pp.126.2.485

Yan Y, Wei CL, Zhang WR, Cheng HP, Liu J (2006) Cross-talk between calcium and reactive oxygen species signaling. Acta Pharmacol Sin 27:821–826. https://doi.org/10.1111/j.1745-7254.2006.00390.x

Yang SY, Lin WY, Hsiao YM, Chiou TJ (2024) Milestones in understanding transport, sensing, and signaling of the plant nutrient phosphorus. Plant Cell 36:1504–1523. https://doi.org/10.1093/plcell/koad326

Zhang K, Li J, Zhou Z, Huang R, Lin S (2021) Roles of alkaline phosphatase *PhoA* in algal metabolic regulation under phosphorus-replete conditions. J Phycol 57:13151. https://doi.org/10.1111/jpy.13151

Authors and Affiliations

Yulia Yugay[1] · Olesya Kudinova[1] · Elena Vasyutkina[1] · Peter Adedibu[2] · Dina Rudenko[1] · Egor Alaverdov[1] · Tatiana Rusapetova[1] · Alexandra Fialko[1] · Veronika Degtyareva[1] · Victor Bulgakov[1] · Larissa Balabanova[3] · Yury Shkryl[1]

✉ Yulia Yugay
 yuya1992@mail.ru

[1] Federal Scientific Center of the East Asia Terrestrial Biodiversity of the Far East Branch of Russian Academy of Sciences, 159 Stoletija Str, Vladivostok 690022, Russia

[2] School of Advanced Engineering Studies "Institute of Biotechnology, Bioengineering and Food Systems", FEFU, 10 Ajax Bay, 690922 Vladivostok, Russia

[3] G.B. Elyakov Pacific Institute of Bioorganic Chemistry, Far Eastern Branch, Russian Academy of Sciences, Prospect 100-Letya Vladivostoka 152, 690022 Vladivostok, Russia